Accepted Manuscript

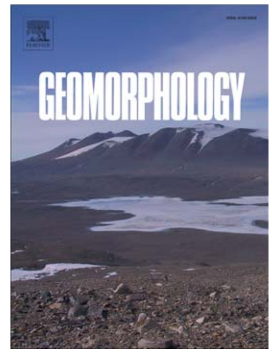

Geomorphic response detection and quantification in a steep forested torrent

Nejc Bezak, Dejan Grigillo, Tilen Urbančič, Matjaž Mikoš, Dušan Petrovič, Simon Rusjan

PII: S0169-555X(16)30512-8
DOI: doi: 10.1016/j.geomorph.2016.06.034
Reference: GEOMOR 5665

To appear in: *Geomorphology*

Received date: 12 November 2015
Revised date: 22 June 2016
Accepted date: 24 June 2016

Please cite this article as: Bezak, Nejc, Grigillo, Dejan, Urbančič, Tilen, Mikoš, Matjaž, Petrovič, Dušan, Rusjan, Simon, Geomorphic response detection and quantification in a steep forested torrent, *Geomorphology* (2016), doi: 10.1016/j.geomorph.2016.06.034

Geomorphic response detection and quantification in a steep forested torrent

Nejc Bezak[a,], Dejan Grigillo[a], Tilen Urbančič[a], Matjaž Mikoš[a], Dušan Petrovič[a], Simon Rusjan[a,*]

Affiliation

[a]Faculty of Civil and Geodetic Engineering, University of Ljubljana, Jamova cesta 2, SI-1000 Ljubljana, Slovenia

E-mail addresses

nejc.bezak@fgg.uni-lj.si; dejan.grigillo@fgg.uni-lj.si; tilen.urbancic@fgg.uni-lj.si; matjaz.mikos@fgg.uni-lj.si; dusan.petrovic@fgg.uni-lj.si; simon.rusjan@fgg.uni-lj.si.

*Corresponding author. Tel.: +386 1 425 40 52; fax: +386 1 251 98 97.

E-mail address: simon.rusjan@fgg.uni-lj.si.

Abstract

Extreme events such as flash floods and debris flows are frequent phenomena that occur in steep torrential catchments; these kinds of events can cause notable geomorphic changes. Repeated terrestrial laser scanning (TLS) surveys were performed in a steep forested catchment of the Kuzlovec torrent (drainage area ~ 0.7 km^2) in central Slovenia, where a ~200-m long section of the torrent was scanned in 2013, 2014, and 2015. The main aim of this study was to perform the geomorphic response detection in the torrent due to hydro-meteorological events of different magnitudes. After applying several pre-processing steps, digital terrain models (DTMs) with a cell resolution of 5 cm were produced. The geomorphic change detection was performed using the DTM of Difference approach (DoD). Several above-average flow events occurred in the period from 2013 to 2015 (some of them can be regarded as floods). The 2014 August extreme flash flood that was initiated by the rainfall event with a return period exceeding 100 years, where maximum 1-minute rainfall intensities were up to 288 mm/h, led to erosion rates of an order of magnitude higher than average annual erosion rates.

Moreover, the analysis of the geomorphic changes shows that the August 2014 flash flood caused intense sediment transport processes that resulted in the changes at the location of the main stream channel thalweg and reduced channel roughness. The unit stream power for the scanned section of the torrent was assessed to be approximately 500 W/m^2 during this extreme event. This is above the thresholds that were suggested to differentiate between the situations where significant geomorphic changes can occur and the situations where geomorphic changes are not notable.

Highlights

-Repeated TLS surveys were performed to detect geomorphic changes

-The flash flood changed the geomorphic characteristics of the torrent channel

-Erosion rates due to the flash flood event were much higher than average annual rates

-High spatial resolution data are a useful tool to detect changes in steep forested torrents

Keywords

Geomorphic change detection; Sediment budget; Flash flood; Headwater geomorphology; Terrestrial laser scanning (TLS)

1 INTRODUCTION

Extreme events such as flash floods and debris flows that are rainfall-triggered can cause large economic losses and even endanger human lives (e.g., Marchi et al., 2009; Mikoš et al., 2004; Rusjan et al., 2009). Severe hydro-meteorological events cause intense soil erosion, sediment transport and deposition processes (e.g., Lenzi and Marchi, 2000); such events occur in the Alpine catchments that were investigated in the scope of the SedAlp project (http://www.sedalp.eu/index.shtml).

Measurements of suspended load and bed load can be performed using various techniques. Some of these can be used for normal and extreme conditions, while other methods for measurements in extreme conditions are more complicated. Direct measuring techniques (e.g., bottle sampling or optical methods) are often used for suspended sediment measurements at catchments of different scales (e.g., Bezak et al., 2015a). In some situations some of these methods are not suitable for determining long-term sediment loads in small mountain catchments because the most extreme events can be missed (Carrivick et al., 2013). For example, manual bottle sampling is very difficult during extreme events. Measurements of bed material transport can often be complicated (e.g., Anderson and Pitlick, 2014), while sediment measurements using direct conventional methods can underestimate the long-term average rates (Carrivick et al., 2013; Kirchner et al., 2001). However, permanent measuring stations such as the Rio Cordon station (e.g., Lenzi and Marchi, 2000; Mao and Lenzi, 2007; Picco et al., 2012) yield valuable information about the long-term sediment budgets and can yield adequate measuring results under normal and extreme conditions. On the other hand, repeated topographic surveys can be used for indirect measurements of sediment transport (sediment budgets) (e.g., Blasone et al., 2014; Theule et al., 2012; Wheaton et al., 2010). Based on the gathered information, the short-term to long-term rates can be determined depending on the number of the surveys and their frequency (Lane et al., 1995; Brasington et al., 2003; Church, 2006). Using this method, various events of different magnitudes can be observed. Different methods such as aerial photogrammetry, airborne LiDAR, and airborne narrow-beam terrestrial-aquatic green can be applied to detect geomorphic changes (Croke et al., 2013; Grove et al., 2013; Mikoš et al., 2005; Tomczyk and Ewertowski, 2013;

Wheaton et al., 2010). The selection of the technique depends on the scale and properties of the investigated area, such as slope and vegetation cover. The identification of the geomorphic changes at the catchment scale can be performed using terrestrial laser scanning (TLS) (e.g., Blasone et al., 2014; Carrivick et al., 2013; Lisenby et al., 2014; Picco et al., 2013; Vericat et al., 2014).

The main aim of this study was to detect geomorphic changes in the torrent following the hydro-meteorological events of different magnitudes. The specific aims of this study were as follows: (i) production of the DTM based on the repeated topographic surveys using terrestrial laser scanning (TLS); (ii) calculation of the DTM of Difference (DoD) maps with the consideration of uncertainty; (iii) analysis of the hydro-meteorological events that caused the largest percentage of changes in the DoD maps; (iv) investigation of the geomorphic changes in the steep forested torrent.

2 DATA AND METHODS

2.1 Case study description

Repeated topographic surveys were performed in 2013, 2014, and 2015 in the steep and forested Kuzlovec torrent, which is part of the Gradaščica River catchment in central Slovenia. Fig. 1 shows the location of the investigated Gradaščica River catchment down to the Dvor gauging station, and the location of this catchment on the map of Slovenia. In the investigated Kuzlovec torrent (Fig. 1), several hydro-meteorological processes are being observed since 2013 (Bezak et al., 2013). Precipitation is recorded at 7 locations around the Kuzlovec torrent using tipping bucket rain gauges. Water level depths and turbidity are measured at the outlet of the Kuzlovec torrent, and an optical disdrometer (Črni Vrh; Fig. 1) is used for observing rainfall characteristics such as raindrop size distribution; the measured rainfall amounts are available in real time online (http://ksh.fgg.uni-lj.si/avp/DisCrniVrh/). Rainfall data measured by the meteorological radar (the spatial resolution of the radar data is 1 km^2) and the rain gauge, which are located at the Črni Vrh nad Polhovim Gradcem and are operated by the Slovenian Environment Agency, were also used in this study. The distance between the Črni Vrh nad Polhovim Gradcem and the Kuzlovec torrent is about 4 km.

Table 1 shows some basic characteristics of the investigated Kuzlovec torrent; forest is the dominant land-use type, and steep slopes predominate for the greater part. The relief in the Gradaščica catchment has been shaped predominantly by fluvial erosion; narrow valleys and steep slopes can be found in the headwater parts (north and north-western parts of the watershed), whereas towards south and south-east the valley widens and the area has prevailing lowland topographical characteristics. The Kuzlovec experimental catchment is located in the headwater, mountainous part of the Gradaščica catchment. Both fluvial and karstic morphologic features can be found in the area. The elevation in the Gradaščica catchment (Fig. 1) ranges from 340 to 1020 m.a.s.l. Valley bottoms are covered by medium to thick layers of alluvial deposits.

Position of the Gradaščica catchment in the Alpine-Dinaric barrier is responsible for high rainfall amounts (yearly averages between 1600 and 1800 mm of rainfall). The highest rainfall totals are observed in autumn and high rainfall amounts are also observed during summer. The Gradaščica River and the Kuzlovec torrent have a rain–snow regime where the highest stream discharges can be usually observed during the autumn rainy period and in early spring as a consequence of snowmelt. Moreover, high discharges can also be measured during summer storms that occur mostly in July and August.

Figure 1: The location of the Kuzlovec torrent in the Gradaščica River catchment and the measuring equipment

Table 1: Basic characteristics of the investigated Kuzlovec torrent

Characteristic/Catchment	Kuzlovec
Catchment area [km^2]	0.71
Elevation range (min; max; mean) [m.a.s.l.]	394; 847; 631
Slope (max; average) [°]	46.5; 27.3
Length of the main stream [km]	1.3
Mean channel slope [%]	23.5
Dominant land-use type	Mixed forest (38%) and broad-leaved forest (44%)

Dominant soil type (FAO type)	Rendzic Leptosol

2.2 TLS and DTM production

To detect geomorphic changes, a geodetic network was established in the Kuzlovec torrent where repeated TLS surveys were performed. The detected ground points in the TLS point clouds were used to interpolate DTM from each survey data, and the precisions of the derived DTMs were evaluated.

2.2.1 Geodetic network

To provide uniform georeferencing for all repeated TLS surveys, a geodetic network was established in the Kuzlovec torrent in 2013. Geodetic datum was defined with 5 GNSS points (points 7, 9, 10, 11, and 12 in Fig. 2), measured and transformed in the national coordinate system (Fig. 2). The geodetic network includes 29 points (Fig. 2) and provides the reference system for the point cloud coordinates. The geodetic network was observed using the sets of angles measuring method and adjusted separately for horizontal and vertical coordinates with 5 GNSS fixed points. All geodetic network points were used in the TLS point cloud georeferencing process as control points.

Figure 2: Geodetic network, locations of control points for the TLS point cloud georeferencing and displacements of geodetic network points between 2013 and 2015

For the geodetic datum of the re-measured geodetic network in 2014 and 2015, we again used all 5 GNSS points (Fig. 2). All these points were established on stable terrain. The average precisions of the adjusted geodetic network points' coordinates for all three measurements are shown in Table 2. Several points along the Kuzlovec torrent, which were destroyed during the several high flow events that occurred in the period between measurements, were re-established during field measurements in 2014 and 2015. Only four points (3a, 3b, 4, and 4a) of the original geodetic network were still detectable in the area scanned in 2014 and 2015; yet, those four points were also shifted. The horizontal displacements of these four points, i.e., between the measurements in 2013 and those in

2015, were calculated as the differences of the adjusted geodetic network points' coordinates and are shown with arrows on the hill-shaded terrain in Fig. 2.

Table 2: The average precision of geodetic network points' coordinates (σ_e, σ_n, σ_H)

Year	σ_e [mm]	σ_n [mm]	σ_H [mm]
2013	1.9	3.2	5.9
2014	2.1	3.1	6.1
2015	2.0	3.2	6.1

2.2.2 TLS data acquisition

Three sets of TLS surveys were undertaken in the Kuzlovec torrent, i.e., in April 2013, August 2014, and March 2015, to identify the geomorphic changes. In 2013, ~600 m of the torrent was scanned between approximately 500 m a.s.l. to the torrent mouth (394 m a.s.l.) with the longitudinal slope of the torrential channel ~18% (Fig. 3-a). At the beginning of February 2014, an extreme sleet event caused extensive damage to the trees; the sleet event was followed by the August 2014 flash flood (Fig. 3-b). Soon after the August 2014 flash flood, large woody debris was removed from the lower reach of the torrent channel by using forest machinery. Consequently, the lower reach of the torrent was heavily modified and could not be included into further analysis (Fig. 3-c). Due to human interventions in the torrent (i.e., the construction of an access forest road), the TLS surveys in 2014 and 2015 were carried out only at the upper part of the torrent (to the forest road end) in a distance of ~200 m with a longitudinal slope of ~23%. The reach of the torrent scanned in 2014 and 2015 is shown in Fig. 2 as a hill-shaded terrain. Table 3 shows the basic characteristics of the TLS surveys performed in 2013, 2014, and 2015 (the number of scan station, the number of all points acquired by the TLS survey, the number of ground points after filtering the original point cloud (filtering is described in section 2.2.3), the global point density of the ground points, and the time of the field work for the TLS data acquisition).

Figure 3: The lower reach of the Kuzlovec torrent in 2013 (a), after the flash flood event in August 2014 (b), and with the road constructed for large wood removal (c)

Table 3: Basic characteristics of the TLS surveys where "Pts surveyed" is the number of all points acquired by the TLS survey, "Ground pts" represent the number of ground points after filtering the original point cloud and "Pts ρ" is the global point density of the ground points.

Year	Scan stations	Pts surveyed	Ground pts	Global ground pts ρ [pts/m^2]	Time of field work [h]
2013	29	443,137,895	16,408,992	1484.2	36
2014	13	258,806,158	7,112,110	1767.4	12
2015	12	224,728,928	7,855,166	1695.9	10

The TLS data were acquired using the terrestrial laser scanner RIEGL VZ-400. In 2013 also the digital camera Nikon D700 was mounted to the scanner. Some of the scanning parameters varied due to the different areas scanned in 2013 and 2014/2015. The scanning in 2013 was performed from 29 scan stations with a resolution of 4 cm at a 50-m distance. In 2014 and 2015 we increased the scanning resolution to 1 cm at a 20-m distance. By analysing the differences in DTMs from 2013 and 2014 we learned that the use of the same positions for the scan stations is very important to avoid false changes in the terrain due to scanning “shadows”. Therefore, in 2014 and 2015 we used 13 and 12 scan stations, respectively. It was not possible to use exactly the same scan stations because of the small landslide that occurred in the interim period. The scans captured from different scan stations in all measurements were registered using tie points, signalized with RIEGL’s cylindrical retro-reflected targets with a height and radius of 10 cm. The points of the geodetic network were signalised with RIEGL’s flat retro-reflected targets with a diameter of 5 cm and used as control points for georeferencing. The absolute precisions of the georeferenced point clouds (σ_{GEO}) were 3.5 cm, 1.5 cm, and 1.2 cm for the measurements in 2013, 2014, and 2015, respectively.

2.2.3 DTM production

Due to terrain's extreme complexity (presence of displaced rocks, coarse channel sediment and large woody debris), special attention was given to DTM production. The same procedure was used to produce DTMs out of the georeferenced point clouds for all three surveys. We used Riegel’s RiSCAN

PRO for manipulating the point cloud and rapidlasso's LAStools for filtering the non-ground points and DTM interpolation. In order to obtain the appropriate amount of data for processing on a common PC, the point clouds were divided into sectors with a length up to 50 m in the longitudinal direction. Each sector was exported from RiSCAN PRO as a LAS file and processed in LAStools. Lasground tool was used for bare-earth extraction. In lasground we used the extra_fine parameter to intensify the search for initial ground points, the step parameter with a value of 0.5, the spike parameter with threshold 0.1 m at which spikes get removed, and offset 0.1 to which points above the current ground estimate get included. The values of the parameters were obtained empirically based on the visual examination of the results. Ground points were imported into RiSCAN PRO and visually inspected. Some non-ground points, which occurred mostly at the edges of the sectors, were removed manually. Each sector of ground points was filtered using octree filter with an increment of 0.02 m. Afterward, all sectors' ground points were merged into a single file and clipped with the 10 m buffer produced out of the torrent profile measured by tachymeter in 2014. Finally, the DTM with the 0.05 m grid-cell size was interpolated using LAStools' las2dem. Further details on the identification of large wood and its accumulation in torrential channels can be found in Grigillo et al. (2015).

2.2.4 Thresholds determination

The geomorphic change detection in the Kuzlovec torrent was performed using the DTM of difference (DoD) approach, described in section 3.2. In order to correctly identify the uncertainty in the derived DoD maps and identify the actual surface changes from the inherent noise, the uncertainty threshold for each DoD was determined. The uncertainty threshold is the minimum level of detection threshold. Predicted elevation changes that occur beneath that threshold are typically discarded, whereas elevation changes above the threshold are treated as real (Wheaton et al., 2010). Two approaches to evaluate the uncertainty were used: uniform threshold and fuzzy inference system approach (FIS). The description of the uniform uncertainty threshold derivation is given in this section and the FIS approach is described in section 2.2.5.

For the uniform threshold determination, we considered the precisions of both DTMs used. Rengers and Tucker (2015) considered the precision of the GPS measurements, the accuracy of the laser scanner, and the precision of the point cloud registration to calculate the total uncertainty of the measured points. We used a similar approach for computing the precisions of point cloud coordinates. To evaluate the precision of DTM we additionally analysed the precisions of the DTM's elevations, which were computed by interpolating the ground points into a grid cell.

For calculating the precision of point cloud coordinates we considered:

(a) the precision of geodetic network points' coordinates σ_e, σ_n, σ_H,

(b) error estimation of the control point signalization σ_{SIG} = 1.5 mm,

(c) the accuracy of terrestrial laser scanning m_{SCAN} = 5 mm (RIEGL, 2014),

(d) the precision of point cloud registration σ_{GEO}.

The precisions of the point cloud coordinates were calculated as:

$$\sigma_{e-CLOUD} = \sqrt{\sigma_e^2 + \frac{\sigma_{SIG}^2}{3} + \frac{m_{SCAN}^2}{3} + \frac{\sigma_{GEO}^2}{3}}, \quad (1)$$

$$\sigma_{n-CLOUD} = \sqrt{\sigma_n^2 + \frac{\sigma_{SIG}^2}{3} + \frac{m_{SCAN}^2}{3} + \frac{\sigma_{GEO}^2}{3}}, \quad (2)$$

$$\sigma_{H-CLOUD} = \sqrt{\sigma_H^2 + \frac{\sigma_{SIG}^2}{3} + \frac{m_{SCAN}^2}{3} + \frac{\sigma_{GEO}^2}{3}}. \quad (3)$$

The results are shown in Table 4.

Table 4: The precision of the point cloud coordinates.

Year	$\sigma_{e\text{-}CLOUD}$ [mm]	$\sigma_{n\text{-}CLOUD}$ [mm]	$\sigma_{H\text{-}CLOUD}$ [mm]
2013	20.3	20.5	20.8
2014	9.5	9.8	10.9
2015	7.8	8.3	9.7

Furthermore, the influence of the bilinear interpolation method used for the DTM creation was considered. Bilinear interpolation identifies the four nearest points to the location of the grid point of an output cell. This is a resampling method that uses the distance-weighted average of the four nearest point elevations to estimate a new elevation for each cell in the grid output. The new interpolated elevation H is calculated as (Chang, 2006):

$$H\left(e,n\right)=a_0+a_1X+a_2Y+a_3XY \tag{4}$$

Where coefficients in Eq. (4) were determined using the coordinates $\left(e,n,H\right)$ of four nearest points:

$$a_0=H_1 \tag{5}$$
$$a_1=H_2-H_1 \tag{6}$$
$$a_2=H_4-H_1 \tag{7}$$
$$a_3=H_1+H_3-H_2-H_4 \tag{8}$$
$$X=\frac{e-e_1}{e_2-e_1} \tag{9}$$
$$Y=\frac{n-n_1}{n_2-n_1} \tag{10}$$

The precisions of the interpolated elevations were calculated using the variance and covariance propagation (Mikhail and Ackermann, 1976). For each point cloud, calculations were carried out on a smaller area of 2×2 m with a 5-cm cell size using partial derivatives of Eq. (4), point cloud coordinates, and their precisions (Table 4):

$$\sigma_{DTM}^2=\left(\frac{\partial H}{\partial H_1}\right)^2\sigma_{H_1}^2+\left(\frac{\partial H}{\partial H_2}\right)^2\sigma_{H_2}^2+\left(\frac{\partial H}{\partial H_3}\right)^2\sigma_{H_3}^2+\left(\frac{\partial H}{\partial H_4}\right)^2\sigma_{H_4}^2+\left(\frac{\partial H}{\partial e_1}\right)^2\sigma_{e_1}^2+\left(\frac{\partial H}{\partial e_2}\right)^2\sigma_{e_2}^2+\left(\frac{\partial H}{\partial n_1}\right)^2\sigma_{n_1}^2+\left(\frac{\partial H}{\partial n_2}\right)^2\sigma_{n_2}^2 \tag{11}$$

The mean values of the precisions of the interpolated elevations were used as the precisions of the individual DTMs (σ_{DTM}) and have the degree of confidence one sigma (Table 5).

Table 5: The precisions of individual DTMs.

	2013	2014	2015
σ_{DTM} [mm]	35.8	18.4	16.1

In the case of precise measurements for detecting and quantifying movements of the points, the appropriate level of confidence should be determined. Generally, the 3-sigma value provides a 99.7% level of confidence (Wolf and Ghilani, 1997; Caspary, 2000). Consequently, the uncertainty threshold of the DoD was calculated using the precisions of the DTMs (Table 5) and the 3-sigma rule as:

$$\text{threshold}_{13-14} = 3\sqrt{\sigma^2_{DTM-13} + \sigma^2_{DTM-14}}, \quad \text{threshold}_{14-15} = 3\sqrt{\sigma^2_{DTM-14} + \sigma^2_{DTM-15}}. \tag{12}$$

The calculated thresholds are 12.1 cm and 7.3 cm for the DoDs from 2013-2014 and 2014-2015, respectively.

2.2.5 FIS uncertainty estimation

Another method used in this study to estimate the elevation uncertainty relies on the Fuzzy Inference System (FIS). FIS enables the estimation of the spatial variable elevation uncertainty in the individual DTMs (Wheaton et al., 2010) and therefore allows discriminating real changes from noise in the assessment of geomorphic changes and estimation of erosion and deposition volumes (Blasone et al., 2014). Fig. 4 and Table 6 show the FIS functions and input rule system used in this study. Point densities were derived from the ground points of each survey and the slopes were calculated from the corresponding DTMs. The basis for the FIS shown in Fig. 4 and Table 6 was FIS that was designed specifically for the TLS data processing and is available in the FIS DEM Error Repository (Bailey, 2016). The repository is part of the Geomorphic Change Detection (GCD) Software (Wheaton, 2016) Version 6.X. The FIS functions were modified in accordance with the characteristics of our TLS surveys and the derived DTMs (Fig. 4 and Table 6). The GCD software was used for the development of FIS functions and spatially variable uncertainty estimation (Wheaton, 2016). More detailed description of the FIS approach can be found in e.g., Bangen et al. (2016), Blasone et al. (2014), and Wheaton et al. (2010). Fig. 5 shows FIS inputs and output rasters for the 2013 and 2014 surveys.

Figure 4: Input and output fuzzy membership functions used in this paper. Inputs: a) slope in degrees and b) point density. Output: elevation uncertainty $\delta(z)$

Figure 5: FIS inputs and output rasters for the 2013-2014 DoD

Table 6: Two-input rule system for estimating elevation uncertainty using the FIS approach.

Rule	Input 1: Slope	Input 2: Point density	Output: $\delta(z)$
1	Low	Sparse	Average
2	Low	Medium	Average
3	Low	High	Low
4	Medium	Sparse	High
5	Medium	Medium	Average
6	Medium	High	Low
7	High	Sparse	High
8	High	Medium	Average
9	High	High	Average

3 RESULTS AND DISCUSSION

3.1 Observed hydro-meteorological conditions

Fig. 6 shows the recorded 20-minute rainfall amounts (from the time of the first TLS survey in April 2013 to the time of the last TLS survey in March 2015) that were observed by one of the tipping buckets located near the Kuzlovec torrent (Fig. 1). The TLS survey dates and the date of occurrence of the relatively extreme sleet event in February 2014 in Slovenia are also shown in Fig. 6. In this period, the tipping bucket rain gauge measured 3,250 mm of rainfall, which means that according to the long-term mean annual rainfall (section 2.1), years 2013, 2014 and 2015 can be regarded as average in terms of hydrological conditions. On the other hand, the summer of 2014 was relatively wet and several relatively extreme events were observed in this period (Fig. 6). Fig. 6 also shows discharge values that were observed at the Kuzlovec torrent water gauging station. One can see that according to the discharge observations, the August 2014 event is several orders of magnitude larger than the other ones. During average flow conditions the discharge at the outlet of the Kuzlovec torrent was between 10 and 15 l/s. Based on the measured rainfall and discharge data, the extreme event that happened in the night from 4 to 5 August 2014 is probably responsible for most of the geomorphic changes in the Kuzlovec torrent (section 3.2). Fig. 7 shows the situation in the Gradaščica River catchment on 5 August 2014, i.e. only a few hours after the extreme event. It can be seen that the August 2014 storm event caused intense soil erosion and sediment transport processes. During the August 2014 event more than 50 shallow landslides were triggered, about 50 km of roads were damaged, and three road bridges were severely damaged in the larger affected area (Fig. 7). The impact of the event was even worse due to the large amounts of damaged and fallen trees in the Gradaščica catchment. This large woody debris was a consequence of an extreme sleet event that occurred in February 2014 in Slovenia and damaged about 40% of Slovenian forests. Forests cover about 60% of the Slovenian territory, and about 500,000 hectares of forests were damaged (SedAlp, 2015b). In some places 80% of the forest was damaged. Moreover, deciduous trees were more affected than coniferous trees (SedAlp, 2015b). The situation after the sleet event in the Kuzlovec torrent is shown in Fig. 8.

Figure 6: Recorded 20-minute rainfall amounts (upper figure) and discharge (lower figure) in the Kuzlovec torrent with dates of the TLS surveys and the sleet event

Figure 7: The situation in the Gradaščica River catchment after the extreme event that occurred in the night from 4 to 5 August, 2014

Figure 8: Consequences of the extreme ice-rain event, in the Kuzlovec torrent, which occurred in Slovenia and damaged about 40% of forests

Highly variable rainfall amounts during the relatively short-term and localized extreme rainfall event were detected by different rainfall gauging instruments. Fig. 9 shows 1-minute rainfall intensities and the accumulated rainfall amounts that were measured using the optical disdrometer during the August 2014 rainfall event (Fig. 1). The total rainfall amount measured by the disdrometer was 185 mm in 9 hours and 40 minutes (1-minute rainfall intensities were up to 288 mm/h, and up to 20,000 rainfall particles were detected). One of the tipping bucket rain gauges measured 140 mm in 9 hours and 20 minutes (Table 7). The accumulated rainfall amount recorded by the meteorological radar from 4 August at 7am to 5 August at 7am was about 100 mm within a period of 10 hours (Table 7). The estimation of the return period of the rainfall event measured by different gauging instruments was based on the intensity-duration-frequency (IDF) curve that was developed for the Črni Vrh nad Polhovim Gradcem (ARSO, 2014). Moreover, the empirical rainfall threshold curves proposed by Caine (1980) and Guzzetti et al. (2008) were used to check whether the observed rainfall event is located above or under the curve that indicates if the event can be regarded as critical in terms of the triggering conditions suitable for initiation of shallow landslides and debris flows. Independently of the measuring instrument, the August 2014 event can be declared as critical based on the Caine (1980) and Guzzetti et al. (2008) thresholds (Table 7). This could be also confirmed by the field surveys where several shallow landslides were detected but no debris flow events could be observed.

Turbidity observations were performed at the outlet of the Kuzlovec torrent during June 2013 and May 2014 but the measurements were not continuous (SedAlp, 2015a). Using the copula functions the estimated *SSL* for the selected period (June 2013-May 2014) was about 5 t (3.8 t and 6.7 t were 50% confidence intervals) where the information about peak discharge and event precipitation sum was used to estimate the *SSL* values for events when turbidity observations were not performed (SedAlp, 2015a).

Figure 9: One-minute rainfall intensities [mm/h] and accumulated rainfall [mm] measured by the disdrometer located in the Gradaščica River catchment

Table 7: Basic properties of the extreme rainfall event in the night from 4 to 5 August 2014

Instrument	Rainfall amount [mm]	Duration [h]	Mean rainfall intensity [mm/h]	Estimated return period [years]	Empirical rainfall threshold (Caine, 1980)	Empirical rainfall threshold (Guzzetti et al., 2008)
Tipping bucket	140	9.33	15	>250	Above the threshold	Above the threshold
Optical disdrometer	185	9.66	19.2	>250	Above the threshold	Above the threshold

Meteorological radar	100	10	10	50	Above the threshold	Above the threshold

3.2 DTM analysis and identification of geomorphic changes

Based on the three TLS surveys the three DTMs were derived according to the methodology described in section 2.2. Based on these final DTM products, two DTM of Difference (DoD) maps were determined. Fig. 10 shows the derived DoD maps that were determined based on the DTMs from 2013, 2014, and 2015 (section 2.2). The methodology and a GCD package, proposed and developed by Wheaton et al. (2010), were used for estimating uncertainty in the derived DoD maps shown in Fig. 10. A uniform threshold classification of uncertainty was selected whereas the methodology described in section 2.2.4 was used to define the thresholds for the two DoD maps (13-14 and 14-15). The calculated thresholds (a minimum level of detection threshold) were 12.1 cm and 7.3 cm for the DoD maps 13-14 and 14-15, respectively. Additionally, the uncertainty was estimated using the FIS approach that is described in section 2.2.5. Table 8 shows the gross and net DoD budgets for two DoD maps shown in Fig. 10.

Table 8: Overview of the erosion rates estimated from the DoD maps with and without consideration of uncertainty (uniform threshold and spatially variable FIS approach)

		DoD 13-14	DoD 14-15
Gross DoD budget	Erosion [m^3]	674	202
	Deposition [m^3]	229	161
	Gross change [m^3]	-445	-41
Net DoD budget (uniform threshold)	Erosion [m^3]	601	172
	Deposition [m^3]	204	127
	Net change using uniform uncertainty threshold [m^3]	-397	-45
Net DoD budget (FIS approach)	Erosion [m^3]	609	156
	Deposition [m^3]	192	116
	Net change using the FIS approach [m^3]	-417	-40

Figure 10: The DoD maps [metres] with the location of the main stream channel thalweg in 2013 and 2014 for a small section of the Kuzlovec torrent

One can notice that the net DoD budget for the DoD 13-14 is almost an order of magnitude greater than the net DoD budget 14-15 (Table 8 and Fig. 10). This applies for the gross and net budgets assessed by both, the uniform threshold and FIS approach (Table 8). The results shown in Fig. 10 indicate that most of the geomorphic changes between 2013 and 2014 occurred near the stream channel or in the channel itself. The location of the stream channel detected in 2013 and 2014 (before and after the flash flood) is shown in Fig. 10. The analysis of the stream channel location during the 2015 survey disclosed only negligible changes in the channel position compared to the 2014 survey. Most of the cells with positive DoD 13-14 values (deposition) can be attributed to the local deposition of sediments. The main Kuzlovec channel has many small side tributaries (gullies) that are not active during normal flow conditions but, obviously, have a notable sediment delivery capacity during extreme hydrometeorological events. The example of such a tributary is shown in Fig. 11, where one can see that a lot of sediment was deposited in the local depression. The location of this small tributary is also shown in Fig. 10. On the other hand, the negative values (DoD 13-14; erosion) can mostly be attributed to the intense sediment transport during high water conditions and the resulting channel degradation. Due to the complex topography, sediment connectivity has an important impact on sediment transport (e.g., Borselli et al., 2008; Cavalli et al., 2013; Croke et al., 2005). This means that sediment transport from upstream areas is interrupted in several torrent sections (also in the lower part of the torrent that was not scanned), leading to more intense erosion processes in some torrent sections where the torrent channel bottom reached bedrock. A similar pattern of geomorphic changes can be observed for DoD 14-15 whereas the magnitude of differences is much smaller (Table 8).

Further, the location of various processes such as floodplain depositions or bank failures is non-uniform (Gartner et al., 2015). Fig. 12 shows the cumulative net erosion along the length of the channel for DoD 13-14 and DoD 14-15 (Fig. 10). For DoD 13-14 the cumulative net erosion along the channel length gradually increases (the situation for DoD 14-15 is similar but the magnitude is much smaller), which could indicate that the studied reach can be identified as a sediment source area with only few deposition areas, mainly associated with the lateral inflow of sediments from small tributaries (Fig. 10). During the field survey it was observed that the main sediment deposition area in the Kuzlovec torrent is located before the confluence of the Kuzlovec torrent with the Gradaščica River where the Kuzlovec torrent channel slope decreases substantially (Fig. 13).

Figure 11: Example of local sediment deposition areas caused by a small torrential tributary to the main Kuzlovec stream channel. The left image was taken in 2013 and the right one shows the situation after the extreme August 2014 event

Figure 12: Cumulative net erosion [m^3] along the length of the channel for DoD 13-14 and DoD 14-15 with the mean channel slope from 2014

Figure 13: Deposition area located before the confluence of the Kuzlovec torrent with the Gradaščica River

Precipitation, discharge, and turbidity measurements carried out in the Gradaščica catchment (section 3.1) indicate that the extreme event that happened in the night from 4 to 5 August is responsible for the majority of geomorphic changes detected at a scanned section of the Kuzlovec torrent (Fig. 2). The calculated erosion based on the 13-14 DoD map was approximately 400 m^3 under consideration of uncertainty (spatially uniform threshold) and about 420 m^3 using the spatially variable FIS approach. The steep torrent channel can be regarded as a sediment source area; however, a large percentage of sediments was displaced and re-deposited along the channel (before leaving the catchment). Large variability in magnitudes of hydro-meteorological events can also be identified based on the precipitation and discharge measurements (Fig. 6) and can be confirmed with estimates of the *SSL* values for about 1 year of measurements (June 2013-May 2014) when approximately 5 t of suspended material was transported out of the entire Kuzlovec torrent catchment. Bed load was not included in this estimation; for torrential streams the proportion between bed load and total load can be between 20 and 90% (Lenzi and Marchi, 2000). Notably, this estimated value (5 t ~ 0.1 t/ha/year) can be regarded as relatively low related to the mean annual soil erosion rates at a catchment scale for Slovenia, which can be up to approximately 7 t/ha/year due to high rainfall erosivity and steep slopes (Bezak et al., 2015b; Panagos et al., 2015). It should be noted that in this time period no extreme event happened in the Kuzlovec torrent. Further, various estimated values of suspended material can be obtained by considering different time periods of measurements and using different methodologies for estimating suspended sediment values (Bezak et al., 2015b). This agrees with the large variability in the measured suspended sediment and bed load delivery from the steep forested torrents (e.g., Rickenmann, 1997). The August 2014 extreme event caused sediment transport that considerably exceeded the average annual sediment transport in the Kuzlovec torrent. This is also confirmed by the DoD map that was based on the DTMs from 2014 and 2015 when the calculated erosion values were approximately 10 times smaller than in DoD 13-14 (Table 8). We could argue that the August 2014 extreme event transported the amount of sediments roughly equivalent or even exceeding the 100-year return period, which is in agreement with the estimated rainfall return period. Similarly, also Anderson and Pitlick (2014) found that one extreme event can account for about 80% of all bed transport in a 10-year period or for more than 50% of all transport estimated in more than a 50-year period.

Magilligan (1992) proposed a minimum unit stream power threshold of 300 W/m^2 that generally differentiates between the reaches where large-scale geomorphic change occurred from those where geomorphic changes are more limited (Buraas et al., 2014). The estimated value of the unit stream power for the scanned section (downstream energy slope is above 20%) of the Kuzlovec torrent during the extreme August 2014 event was approximately 500 W/m^2, meaning that this torrent can be regarded as a high-energy torrent. Thus, large-scale geomorphic changes can be expected during such events. Recently Marchi et al. (2015) analyzed stream power of multiple flash flood events with the return period exceeding 100 years that occurred in the mountainous catchments of southern and central Europe. The analyses showed consistency between the unit stream power values, the severity of extreme floods, and the observed geomorphic changes. Further, similar as for the Kuzlovec torrent the bedrock channels showed the highest values of the unit stream power but no significant erosion was detected (Marchi et al., 2015). For the alluvial channels the geomorphic changes were more significant. Surian et al. (2016) analyzed the factors that control or are related to channel widening for six rivers located in the Apennines (Italy) and found that due to the extreme flash flood event (more than a 100-year return period) the channel widening was more explicit at channel reaches with slope <4% than at steeper reaches (slope $\geq$ 4%). It was also found that channel widening is strongly related with the unit stream power whereas the dependence was larger in cases when the unit stream power was calculated with the pre-flood channel width than with the post-flood channel width (Surian et al., 2016).

The Kuzlovec torrent channel longitudinal slope is above 20% in the investigated reach (Fig. 2), and in steep gradient streams, macroscale structures introduce additional flow resistance (Hey, 1988). With regard to mesoscale structures in such streams, different bed morphologies are typical for different slope ranges, as proposed by Grant et al. (1990), Schälchli (1991), Montgomery and Buffington (1997), Chartrand and Whiting (2000), and Weichert et al. (2004). In the Kuzlovec torrent we can see that it is well above the lower limit for steep gradient streams and, therefore, it is of the cascade type as proposed by the aforementioned authors. During large floods different roughness macro and mesoscale structures control the stability of the torrent bed, storage of bed material, and sediment output (Kozlowski and Ergenzinger, 1999). The sediment transport and interrupted sediment connectivity from upstream areas of the Kuzlovec torrent, due to its complex topography and the presence of large amounts of woody debris, affected also more resistant sediment deposits in the Kuzlovec channel, which were in some sections completely washed away, until the water flow disclosed the bedrock. Consequently, along such sections, the roughness in the channel was reduced (i.e., between 2013 and 2014), which probably resulted in higher water velocities.

4 CONCLUSIONS

This paper shows the results of the repeated TLS surveys that were performed in 2013, 2014, and 2015 in a ~200-m long reach of a steep forested torrent, i.e. the Kuzlovec torrent, in central Slovenia. Based on the TLS surveys, the DTMs were derived after applying several pre-processing steps. The DoD approach was used to detect changes in the scanned area; the hydrometeorological events responsible for the changes were analysed. The following conclusions can be drawn based on the presented results:

-The extreme August 2014 flash flood triggered by the rainfall event with a return period of over 100 years had a great impact on the geomorphic conditions in the Kuzlovec torrent. The detected changes affected the location of the main stream channel thalweg and reduced channel roughness.

-Most of the local deposition areas can be attributed to the sediment delivery from small local side tributaries (gullies) whereas the erosion areas detected near the stream channel or in the channel itself are mostly caused by the water flow drag force. A particular torrential channel characteristic is the shifting and degradation of the Kuzlovec torrent channel bed, which is, in some short sub-reaches, eroded to the bedrock.

-The sediment budget due to an extreme flash flood can be more than a magnitude larger than the mean annual budget during average hydrological years.

-Notable differences in the measured rainfall amounts during the extreme event were disclosed by the use of various measuring instruments, i.e., the tipping bucket rain gauge, the optical disdrometer, and the meteorological radar.

-The unit stream power for the investigated area of the Kuzlovec torrent was assessed to be approximately 500 W/m^2 during the August 2014 extreme event. This means that the unit stream power was well above the often used threshold (e.g., Magilligan, 1992).

-DTM with a high spatial resolution is needed to observe geomorphic changes in steep forested torrential areas, such as the Kuzlovec torrent.

Acknowledgments

We wish to thank the Slovenian Environment Agency (ARSO) for providing the data used in this study. The results of the study are part of the Faculty of Civil and Geodetic Engineering's (UL FGG) work within the European research project SedAlp, which is jointly financed by the European Union in the framework of the Alpine Space program and the Slovenian Research Agency (ARRS) within the research program P2-0180 Water Science and Technology, and Geotechnics. The results of the study are also part of the Slovenian national research project No. 590 “Modelling Hydrologic Response of nonhomogeneous Catchments”. The critical and useful comments of an anonymous reviewer, John

Pitlick, Frederic Liebault, and the associate editor improved this work, for which the authors are very grateful.

REFERENCES

Anderson, S., Pitlick, J., 2014. Using repeat lidar to estimate sediment transport in a steep stream. Journal of Geophysical Research: Earth Surface, 119, 621-643.

ARSO, 2014. Return period values for extreme rainfall events. Slovenian Environment Agency, 63 p. (http://meteo.arso.gov.si/met/sl/climate/tables/precip_return_periods_newer/).

Bailey, P., 2016. FIS DEM Error Repository. https://bitbucket.org/pipbailey/fis-dem-error-repository.

Bangen, S., Hensleigh, J., McHugh, P., Wheaton, J., 2016. Error modeling of DEMs from topographic surveys of rivers using fuzzy inference system. Water Resources Research, 52, doi: 10.1002/2015WR018299.

Bezak, N., Rusjan, S., Petan, S., Sodnik, J., Mikoš, M., 2015b. Estimation of soil loss by the WATEM/SEDEM model using an automatic parameter estimation procedure. Environmental Earth Sciences, 74(6), 5245-5261.

Bezak, N., Šraj, M., Mikoš, M., 2015. Analyses of suspended sediment loads in Slovenian rivers. Hydrological Sciences Journal, doi: 10.1080/02626667.2015.1006230.

Bezak, N., Šraj, M., Rusjan, S., Kogoj, M., Vidmar, A., Sečnik, M., Brilly, M., Mikoš, M., 2013. Primerjava dveh sosednjih eksperimentalnih hudourniških porečij: Kuzlovec in Mačkov graben = Comparison between two adjacent experimental torrential watersheds: Kuzlovec and Mačkov graben. Acta hydrotechnica, 26(45), 85-97 (in Slovene).

Blasone, G., Cavalli, M., Marchi, L., Cazorzi, F., 2014. Monitoring sediment source areas in a debris-flow catchment using terrestrial laser scanning. Catena, 123, 23-36.

Borselli, L., Cassi, P., Torri, D., 2008. Prolegomena to sediment and flow connectivity in the landscape: A GIS and field numerical assessment. Catena, 75(3), 268-277.

Brasington, J., Langham, J., Rumsby, B., 2003. Methodological sensitivity of morphometric estimates of coarse fluvial sediment transport. Geomorphology, 53(3-4), 299-316.

Buraas, E.M., Renshaw, C.E., Magilligan, F.J., Dade, W.B., 2014. Impact of reach geometry on stream channel sensitivity to extreme floodss. Earth Surface Processes and Landforms, 39, 1778-1789.

Caine, N., 1980. The rainfall intensity–duration control of shallow landslides and debris flows. Geografiska Annaler Series A-Physical Geography, 62(1-2), 23-27.

Carrivick, J.L., Geilhausen, M., Warburton, J., Dickson, N.E., Carver, S.J., Evans, A.J., Brown, L.E., 2013. Contemporary geomorphological activity throughout the proglacial area of an alpine catchment. Geomorphology, 188, 83-95.

Caspary, W.F., 2000. Concepts of network and deformation analysis. School of Surveying, The University of New South Wales, Kensington.

Cavalli, M., Trevisani, S., Comiti, F., Marchi, L., 2013. Geomorphometric assessment of spatial sediment connectivity in small Alpine catchments. Geomorphology, 188, 31-41.

Chang, K.T., 2006. Introduction to Geographic Information Systems. 3rd ed. Boston: McGrawHill.

Chartrand, S.M., Whiting, P.J., 2000. Alluvial architecture in headwater streams with special emphasis on step-pool topography. Earth Surface Processes and Landforms, 25(6), 583-600.

Church, M., 2006. Bed material transport and the morphology of alluvial river channels. Annual Review of Earth and Planetary Sciences, 34, 325-354.

Croke, J., Mockler, S., Fogarty, P., Takken, I., 2005. Sediment concentration changes in runoff pathways from a forest road network and the resultant spatial pattern of catchment connectivity. Geomorphology, 68(3-4), 257-268.

Croke, J., Todd, P., Thompson, C., Watson, F., Denham, R., Khanal, G., 2013. The use of multi temporal LiDAR to assess basin-scale erosion and deposition following the catastrophic January 2011 Lockyer flood, SE Queensland, Australia. Geomorphology, 184, 111-126.

Gartner, J.D., Dade, W.B., Renshaw, C.E., Magilligan, F.J., Buraas, E.M., 2015. Gradients in stream power influence lateral and downstream sediment flux in floods. Geology, 43(11), 983-986.

Grant, G.E., Swanson, F.J., Wolman, M.G., 1990. Pattern and origin of stepped-bed morphology in high-gradient streams, Western Cascades, Oregon. Geological Society of America Bulletin, 102(3), 340-352.

Grigillo, D., Vrečko, A., Mikoš, M., Gvozdanovič, T., Anžur, A., Vezočnik, R., Petrovič, D., 2015. Determination of large wood accumulation in a steep forested torrent using laser scanning. In: Lollino, Giorgio (ed.). *Engineering Geology for Society and Territory - Volume 3 : River Basins, Reservoir Sedimentation and Water Resources*. Cham: Springer International Publishing, 127-130.

Grove, J.R., Croke, J., Thompson, C., 2013. Quantifying different riverbank erosion processes during an extreme flood event. Earth Surface Processes and Landforms, 38(12), 1393-1406.

Guzzetti, F., Peruccacci, S., Rossi, M., Stark, C.P., 2008. The rainfall intensity–duration control of shallow landslides and debris flows: an update. Landslides, 5(1), 3-17.

Hey, R.D., 1988. Bar form resistance in gravel-bed rivers. Journal of Hydraulic Engineering, 114(12), 1498-1508.

Kirchner, J.W., Finkel, R.C., Riebe, C.S., Granger, D.E., Clayton, J.L., King, J.G., Megahan, W.F., 2001. Mountain erosion over 10 yr, 10 k.y., and 10 m.y. time scales. Geology, 29(7), 591-594.

Kozlowski, B., Ergenzinger, P., 1999. Ring structures - A specific new cluster type in steep mountain torrents. Proceedings of the 28th Congress of the IAHR, Graz, papers on CD-ROM.

Lane, S.N., Richards, K.S., Chandler, J.H., 1995. Morphological Estimation of the Time-Integrated Bed Load Transport Rate. Water Resources Research, 31(3), 761-772.

Lenzi, M.A., Marchi, L., 2000. Suspended sediment load during floods in a small stream of the Dolomites (northeastern Italy). Catena, 39(4), 267-282.

Lisenby, P.E., Slattery, M.C., Wasklewicz, T.A., 2014. Morphological organization of a steep, tropical headwater stream: The aspect of channel bifurcation. Geomorphology, 214, 245-260.

Magilligan, F.J., 1992. Thresholds and the spatial variability of flood power during extreme floods. Geomorphology, 5, 373-390.

Mao, L., Lenzi, M.A, 2007. Sediment mobility and bedload transport conditions in an alpine stream. Hydrological Processes, 21(14), 1882-1891.

Marchi, L., Borga, M., Preciso, E., Sangati, M., Gaume, E., Bain, V., Delrieu, G., Bonnifait, L., Pogacnik, N., 2009. Comprehensive post-event survey of a flash flood in Western Slovenia: observation strategy and lessons learned. Hydrological Processes, 23(26), 3761-3770.

Marchi, L., Cavalli, M., Amponsah, W., Borga, M., Crema, S., 2015. Upper limits of flash flood stream power in Europe. Geomorphology, doi: 10.1016/j.geomorph.2015.11.005.

Mikhail, E.M., Ackermann F.E., 1976. Observations and least squares. IEP-A Dun-Donnelley, New York.

Mikoš, M., Četina, M., Brilly, M., 2004. Hydrologic conditions responsible for triggering the Stoze landslide, Slovenia. Engineering Geology, 73(3-4), 193-213.

Mikoš, M., Vidmar, A., Brilly, M., 2005. Using a laser measurement system for monitoring morphological changes on the Strug rock fall, Slovenia. Natural Hazards and Earth System Sciences, 5(1), 143-153.

Montgomery, D.R., Buffington, J.M., 1997. Channel-reach morphology in mountain drainage basins. Geological Society of America Bulletin, 109(5), 596-611.

Panagos, P., Borrelli, P., Poesen, J., Ballabio, C., Lugato, E., Meusburger, K., Montanarella, L., Alewell, C., 2015. The new assessment of soil loss by water erosion in Europe. Environmental Science & Policy, 54, 438-447. doi:10.1016/j.envsci.2015.08.012

Picco, L., Mao, L., Cavalli, M., Buzzi, E., Rainato, R., Lenzi, M.A., 2013. Evaluating short-term morphological changes in a gravel-bed braided river using terrestrial laser scanner. Geomorphology, 201, 323-334.

Picco, L., Mao, L., Rigon, E., Moretto, J., Ravazzolo, D., Delai, F., Lenzi, M.A., 2012. An Update of the Sediment Fluxes Investigation in the Rio Cordon (Italy) after 25 Years of Monitoring. Journal of Agricultural Engineering, doi: 10.4081/jae.2012.e17.

Rickenmann, D., 1997. Sediment transport in Swiss torrents. Earth Surface Processes and Landforms, 22, 937-951.

Rengers, F.K., Tucker, G.E., 2015. The evolution of gully headcut morphology: a case study using terrestrial laser scanning and hydrological monitoring. Earth Surface Processes and Landforms, 40, 1304-1317.

RIEGL, 2014. Data Sheet, RIEGL VZ-400. Available online at: http://www.riegl.com/uploads/tx_pxpriegldownloads/10_DataSheet_VZ-400_2014-09-19.pdf (Accessed 25 September 2015)

Rusjan, S., Kobold, M., Mikos, M., 2009. Characteristics of the extreme rainfall event and consequent flash floods in W Slovenia in September 2007. Natural Hazards and Earth System Sciences, 9(3), 947-956.

Schälchli, U., 1991. Morphologie und Strömungsverhältnisse in Gebirgsbächen: ein Verfahren zur Festlegung von Restwasserabflüssen. Mitteilungen der Versuchsanstalt für Wasserbau, Hydrologie und Glaziologie, ETH Zürich, No. 113.

SedAlp, 2015a. SedAlp WP5 Report: Sediment transport monitoring, SedAlp Alpine Space. www.sedalp.eu/download/dwd/events/finalConf/WP5_Habersack.pdf

SedAlp, 2015b. SedAlp WP7 Report: Sediment management, SedAlp Alpine Space. www.sedalp.eu/download/dwd/reports/WP7_final_report.pdf

Surian, N., Righini, M., Lucia, A., Nardi, L., Amponsah, W., Benvenuti, M., Borga, M., Cavalli, M., Comiti, F., Marchi, L., Rinaldi, M., Viero, A., 2016. Channel response to extreme floods: Insights on controlling factors from six mountain rivers in northern Apennines, Italy. Geomorphology, doi: 10.1016/j.geomorph.2016.02.002.

Theule, J.I., Liebault, F., Loye, A., Laigle, D., Jaboyedoff, M., 2012. Sediment budget monitoring of debris-flow and bedload transport in the Manival Torrent, SE France. Natural Hazards and Earth System Sciences, 12, 731-749.

Tomczyk, A.M., Ewertowski, M., 2013. Quantifying short-term surface changes on recreational trails: The use of topographic surveys and 'digital elevation models of differences' (DODs). Geomorphology, 183, 58-72.

Vericat, D., Smith, M.W., Brasington, J., 2014. Patterns of topographic change in sub-humid badlands determined by high resolution multi-temporal topographic surveys. Catena, 120, 164-176.

Weichert, R., Bezzola, G. R., Minor, H.-E., 2004. Bed morphology in steep open channels – State-of-the-art and first results of a flume study. Proceedings of the Internationales Symposion Interpraevent 2004, Riva del Garda, Italy, Vol. 3, 343-354.

Wheaton, J.M., Brasington, J., Darby, S.E., Sear, D.A., 2010. Accounting for uncertainty in DEMs from repeat topographic surveys: improved sediment budgets. Earth Surface Processes and Landforms, 35(2), 136-156.

Wheaton, J.M., 2016. Geomorphic change detection software. http://gcd.joewheaton.org/

Wolf, P.R., Ghilani, C.D., 1997. Adjustment computations – Statistics and least squares in surveying and GIS. John Wiley & Sons, New York.

FIGURE CAPTIONS

Figure 1: The location of the Kuzlovec torrent in the Gradaščica River catchment and the measuring equipment

Figure 2: Geodetic network, locations of control points for the TLS point cloud georeferencing and displacements of geodetic network points between 2013 and 2015

Figure 3: The lower reach of the Kuzlovec torrent in 2013 (a), after the flash flood event in August 2014 (b), and with the road constructed for large wood removal (c)

Figure 4: Input and output fuzzy membership functions used in this paper. Inputs: a) slope in degrees and b) point density. Output: elevation uncertainty $\delta(z)$

Figure 5: FIS inputs and output rasters for the 2013-2014 DoD

Figure 6: Recorded 20-minute rainfall amounts (upper figure) and discharge (lower figure) in the Kuzlovec torrent with dates of the TLS surveys and the sleet event

Figure 7: The situation in the Gradaščica River catchment after the extreme event that occurred in the night from 4 to 5 August, 2014

Figure 8: Consequences of the extreme ice-rain event, in the Kuzlovec torrent, which occurred in Slovenia and damaged about 40% of forests

Figure 9: One-minute rainfall intensities [mm/h] and accumulated rainfall [mm] measured by the disdrometer located in the Gradaščica River catchment

Figure 10: The DoD maps [metres] with the location of the main stream channel thalweg in 2013 and 2014 for a small section of the Kuzlovec torrent

Figure 11: Example of local sediment deposition areas caused by a small torrential tributary to the main Kuzlovec stream channel. The left image was taken in 2013 and the right one shows the situation after the extreme August 2014 event

Figure 12: Cumulative net erosion [m^3] along the length of the channel for DoD 13-14 and DoD 14-15 with the mean channel slope from 2014

Figure 13: Deposition area located before the confluence of the Kuzlovec torrent with the Gradaščica River

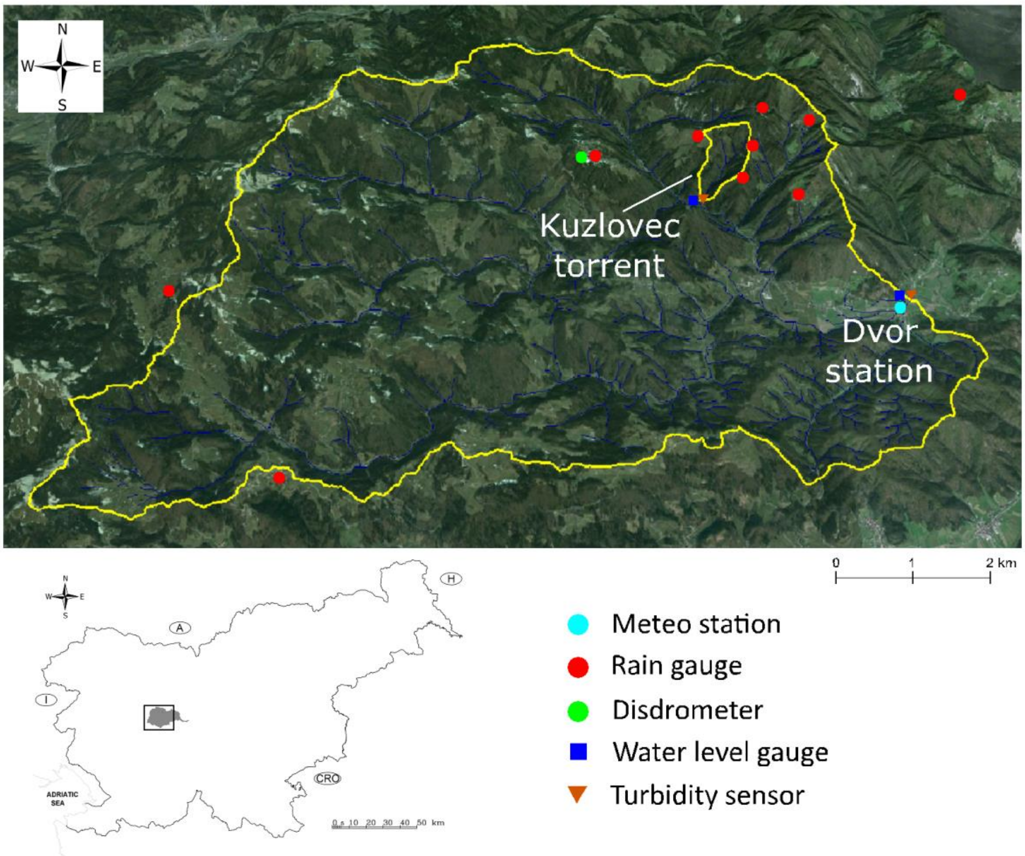

N
W
E
S
Kuzlovec
torrent
Dvor
station
0
1
2 km
A
H
I
CRO
ADRIATIC
SEA
0 5 10 20 30 40 50 km
Meteo station
Rain gauge
Disdrometer
Water level gauge
Turbidity sensor

Fig. 1

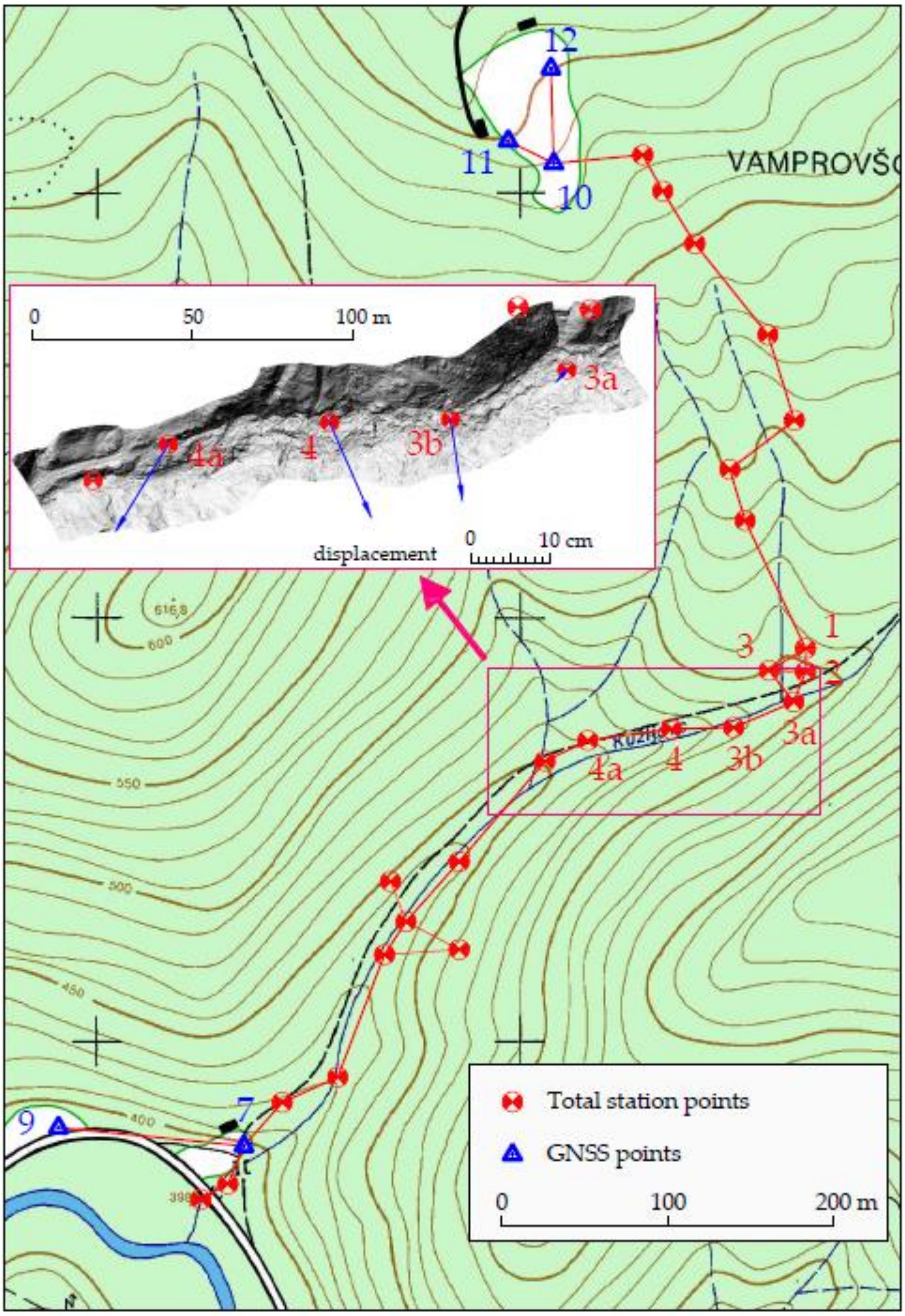

12
11
10
VAMPROVŠ
0
50
100 m
3a
4a
4
3b
displacement
0
10 cm
616,8
600
550
500
450
400
390
1
2
3
3a
4a
4
3b
7
9
Total station points
GNSS points
0
100
200 m

Fig. 2

Fig. 3

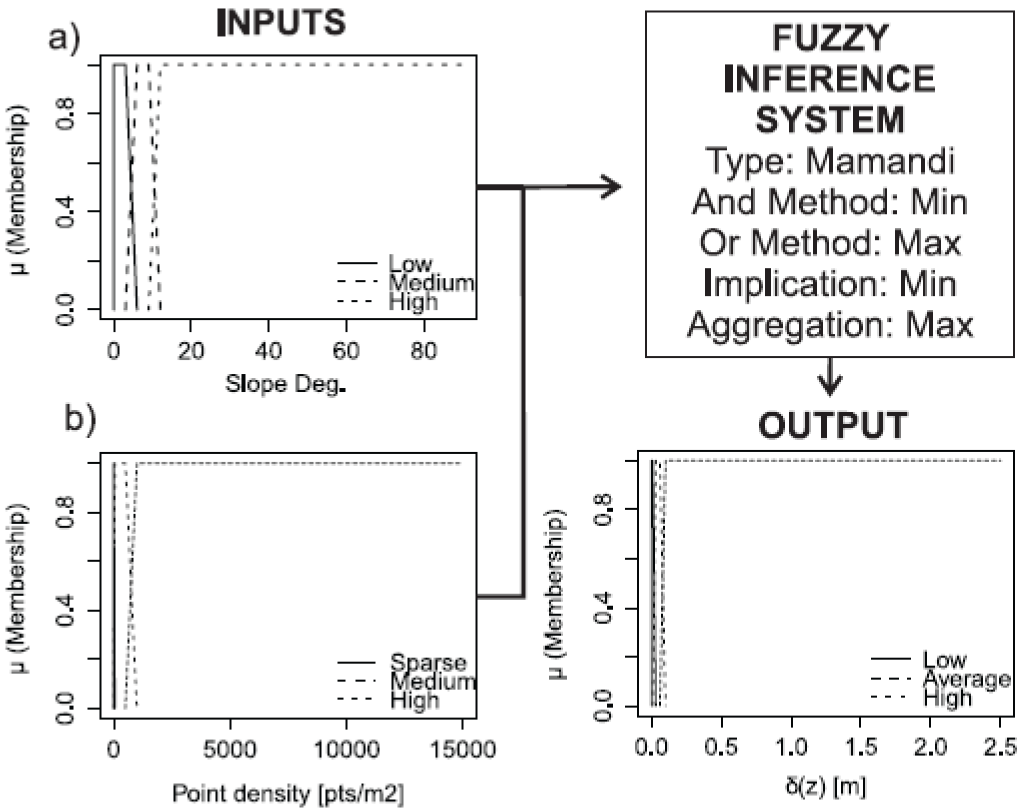
INPUTS
a)
μ (Membership)
0.0
0.4
0.8
Low
Medium
High
0
20
40
60
80
Slope Deg.
b)
μ (Membership)
0.0
0.4
0.8
Sparse
Medium
High
0
5000
10000
15000
Point density [pts/m2]
FUZZY
INFERENCE
SYSTEM
Type: Mamandi
And Method: Min
Or Method: Max
Implication: Min
Aggregation: Max
OUTPUT
μ (Membership)
0.0
0.4
0.8
Low
Average
High
0.0
0.5
1.0
1.5
2.0
2.5
δ(z) [m]

Fig. 4

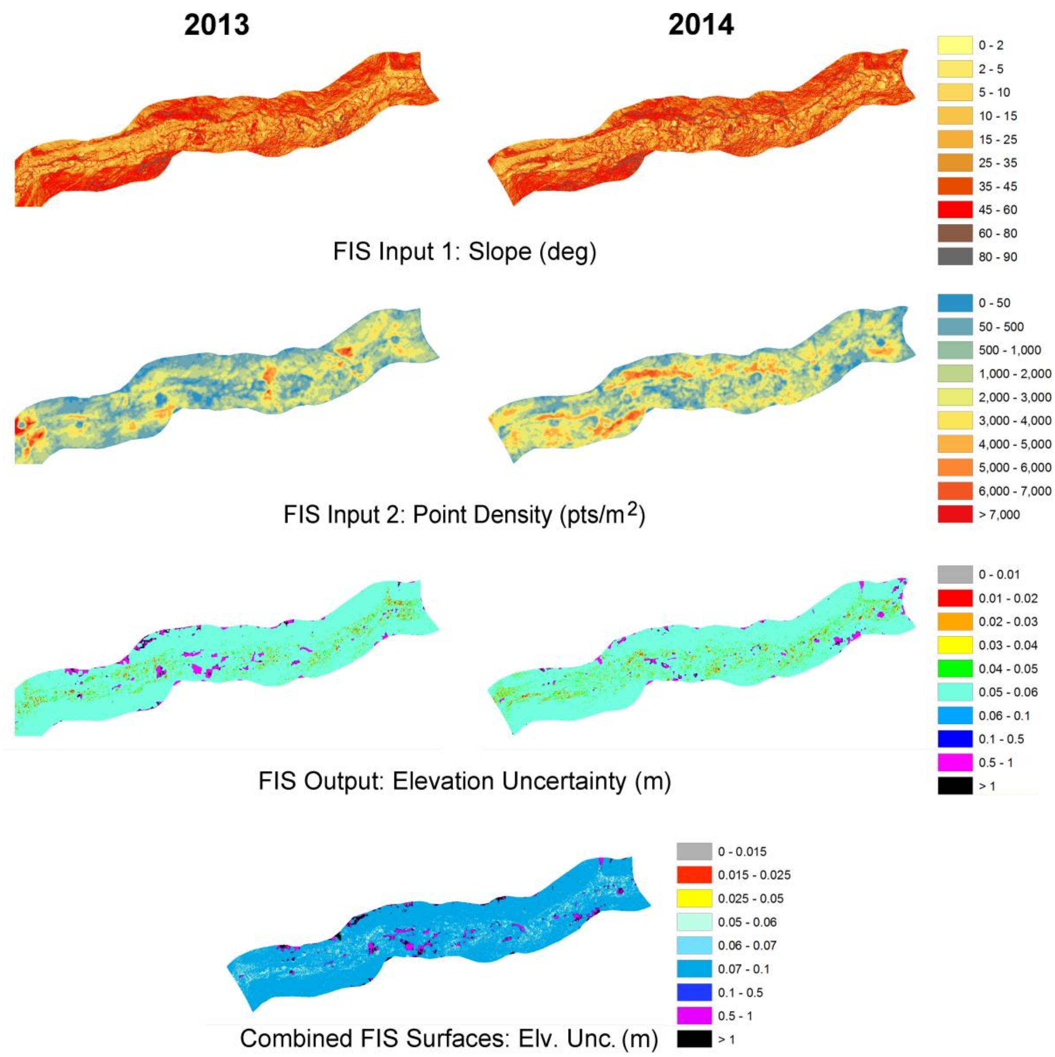
2013
2014
FIS Input 1: Slope (deg)
0 - 2
2 - 5
5 - 10
10 - 15
15 - 25
25 - 35
35 - 45
45 - 60
60 - 80
80 - 90
FIS Input 2: Point Density (pts/m2)
0 - 50
50 - 500
500 - 1,000
1,000 - 2,000
2,000 - 3,000
3,000 - 4,000
4,000 - 5,000
5,000 - 6,000
6,000 - 7,000
> 7,000
FIS Output: Elevation Uncertainty (m)
0 - 0.01
0.01 - 0.02
0.02 - 0.03
0.03 - 0.04
0.04 - 0.05
0.05 - 0.06
0.06 - 0.1
0.1 - 0.5
0.5 - 1
> 1
Combined FIS Surfaces: Elv. Unc. (m)
0 - 0.015
0.015 - 0.025
0.025 - 0.05
0.05 - 0.06
0.06 - 0.07
0.07 - 0.1
0.1 - 0.5
0.5 - 1
> 1

Fig. 5

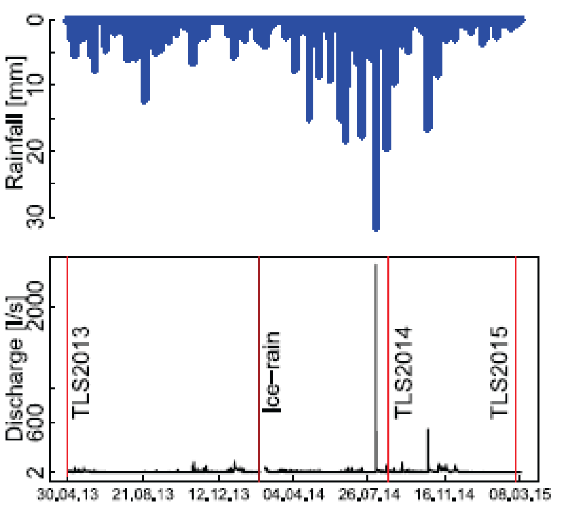
Rainfall [mm]
0
10
20
30
Discharge [l/s]
2000
600
2
TLS2013
Ice-rain
TLS2014
TLS2015
30.04.13
21.08.13
12.12.13
04.04.14
26.07.14
16.11.14
08.03.15

Fig. 6

Fig. 7a

Fig. 7b

Fig. 8

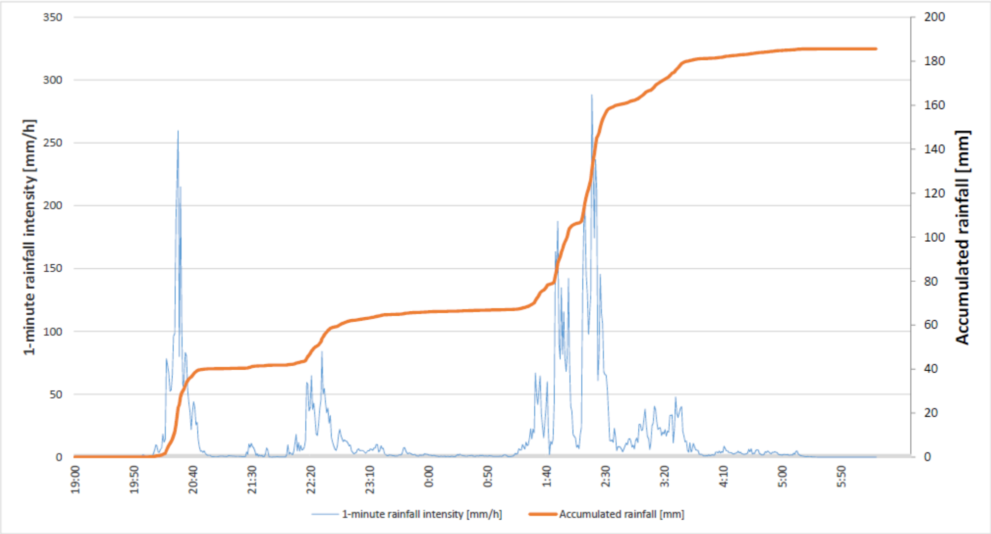
1-minute rainfall intensity [mm/h]
Accumulated rainfall [mm]
350
300
250
200
150
100
50
0
200
180
160
140
120
100
80
60
40
20
0
19:00
19:50
20:40
21:30
22:20
23:10
0:00
0:50
1:40
2:30
3:20
4:10
5:00
5:50
1-minute rainfall intensity [mm/h]
Accumulated rainfall [mm]

Fig. 9

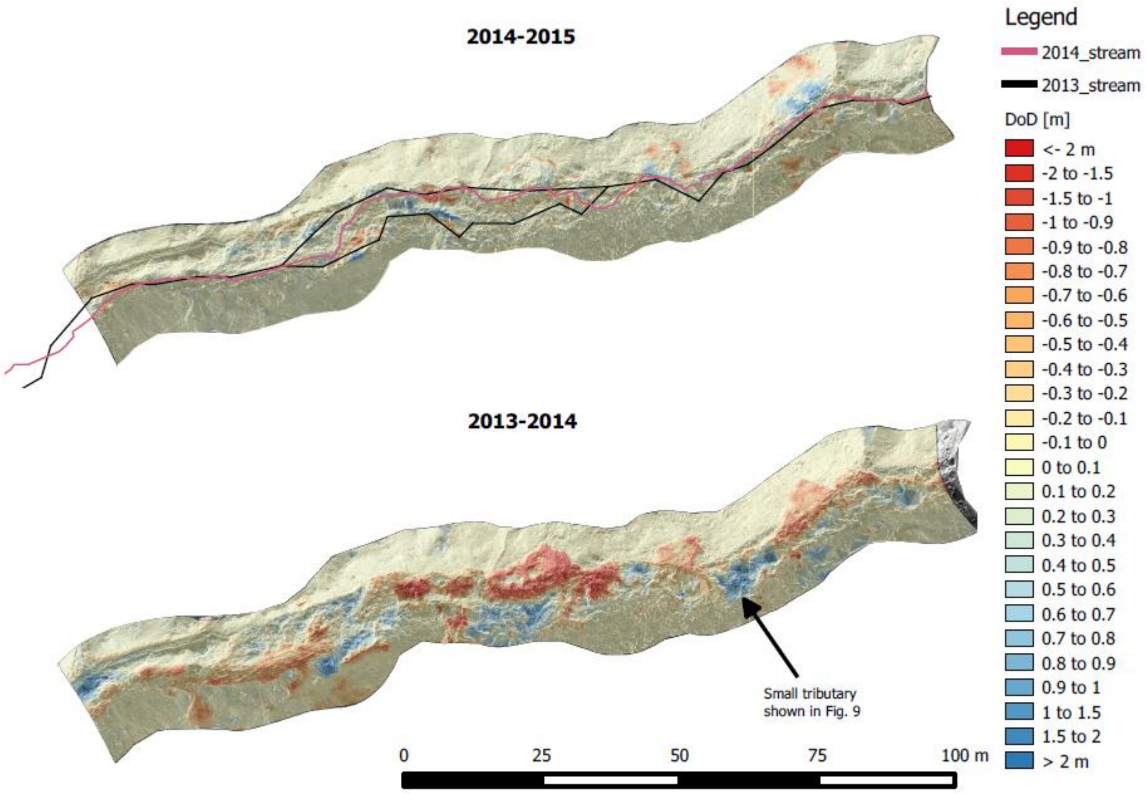

Fig. 10

Fig. 11a

Fig. 11b

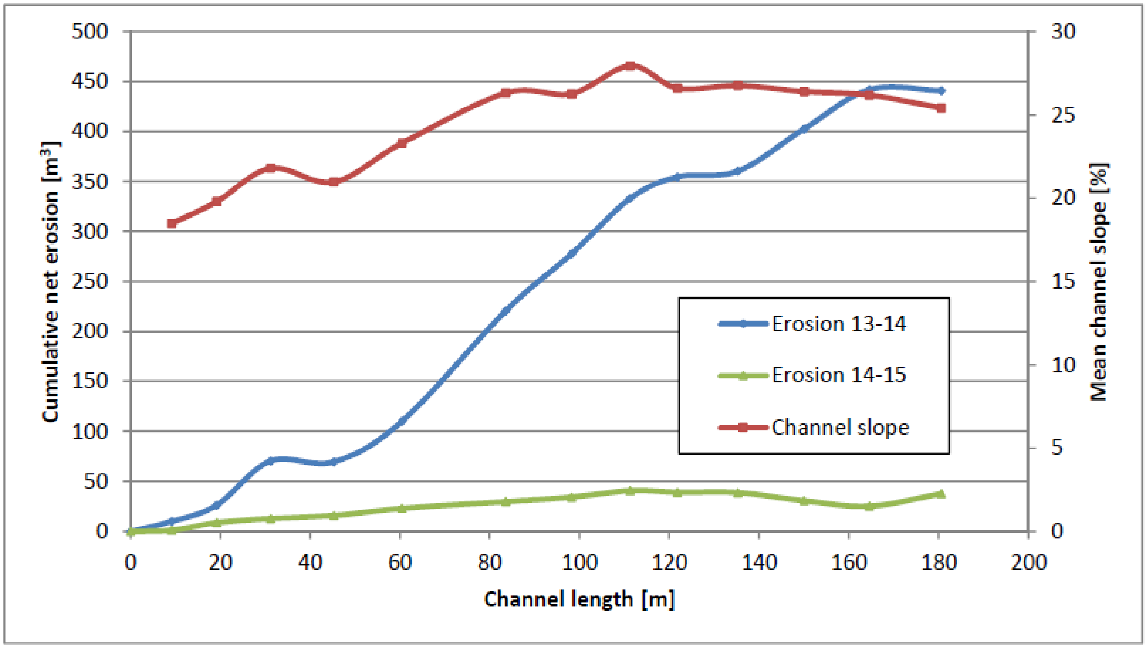

Fig. 12

Fig. 13